Original Article
Discovery of an interplay between the gut microbiota and esophageal squamous cell carcinoma in mice

Man Kit Cheung[1], Grace Gar Lee Yue[2,3], Kei Yin Tsui[1], Adele Joyce Gomes[1], Hoi Shan Kwan[4], Philip Wai Yan Chiu[1], Clara Bik San Lau[2,3]

[1]Department of Surgery, The Chinese University of Hong Kong, Shatin, New Territories, Hong Kong; [2]Institute of Chinese Medicine, The Chinese University of Hong Kong, Shatin, New Territories, Hong Kong; [3]State Key Laboratory of Research on Bioactivities and Clinical Applications of Medicinal Plants, The Chinese University of Hong Kong, Shatin, New Territories, Hong Kong; [4]School of Life Sciences, The Chinese University of Hong Kong, Shatin, New Territories, Hong Kong

Abstract: Esophageal squamous cell carcinoma (ESCC) is the main type of esophageal cancer (EC) worldwide, causing half a million deaths each year. Recent evidence has demonstrated the role of the gut microbiota in health and disease. However, our current understanding of the gut microbiome in EC remains scarce. Here, we characterized the gut and esophageal microbiome in a metastatic mouse model of ESCC and examined the functional roles of the gut microbiota in EC development in fecal microbiota transplantation (FMT) experiments. Nude mice intraperitoneally xenografted with human EC-109 cells showed significant alterations in the overall structure, but not alpha diversity, of the gut and esophageal microbiome as compared to naïve control mice. Xenograft of EC cells depleted the order *Pasteurellales* in the gut microbiome, and enriched multiple predicted metabolic pathways, including those involved in carbohydrate and lipid metabolism, in the esophageal microbiome. FMT of stool from healthy mice to antibiotic-treated xenograft-bearing mice significantly attenuated liver metastasis, suggesting a protective role of the commensal gut microbiota in EC. Moreover, we showed that combination chemotherapy with cisplatin and 5-fluorouracil, and the anti-EC medicinal herb *Andrographis paniculata* (AP) differentially affected the gut and esophageal microbiome in EC. FMT experiment revealed a reduced anti-metastatic efficacy of AP on liver metastasis in antibiotic-treated xenograft-bearing mice, suggesting a role of the commensal gut microbiota in the anti-metastatic efficacy of the herb. In conclusion, our findings reveal for the first time an interplay between the gut microbiota and EC and provide insights into the treatment strategies for EC.

Keywords: Gut microbiota, esophageal cancer, microbiome, fecal microbiota transplantation, dysbiosis, *Andrographis paniculata*, anti-metastasis

Introduction

Esophageal cancer (EC) is the seventh most common and sixth most deadly cancer worldwide, accounting for 572,000 new cases and 509,000 deaths in 2018 [1]. In China, EC represents the fourth most common cause of cancer deaths [2]. Esophageal squamous cell carcinoma (ESCC) is the most common histological subtype of EC worldwide and comprises more than 90% of all EC cases in China [2, 3]. Distant metastasis is the major cause of treatment failure and death in EC [4]. In fact, over 50% of EC patients have either unresectable tumors or radiographically visible metastases at the time

of initial diagnosis [5]. Liver and lung are the most common sites of metastasis in EC [6].

The communities of microbes living in and on the human body - the human microbiota - can affect cancer initiation, progression, and response to therapy [7]. In EC, human microbiome studies conducted to date are on mucosa or tumor samples from the esophagus [8-12], or adjacent stomach or oral samples [13-15]. It is now known that the gut (intestinal) microbiota plays important roles in health and disease, including cancers [16]. These microbes can exert indirect effects on the progression of tumors at distant sites or their response to thera-

py by altering the circulating metabolites, which in turn affects the general host physiology [7]. Until now, there is only one study of the gut microbiome in EC, which was conducted in mice [17]. Therefore, it remains largely unknown how EC affects the gut microbiome and whether the effects are similar to those on the esophageal microbiome. Besides, a previous population-based case-control study demonstrates a dose-dependent positive association between penicillin exposure and the risk of EC [18], suggesting a protective role of the commensal gut microbiota in EC development. However, no definitive functional studies have been performed to examine the causality.

Combination chemotherapy with cisplatin and 5-fluorouracil (5-FU) (CF therapy) is commonly used for patients with unresectable locally advanced or metastatic EC [19]. Cisplatin and 5-FU have been separately shown to alter the gut microbiome in cancers [17, 20]. The effects of their combined use with docetaxel in DCF therapy on the gut microbiome have also been reported [21]. However, the effects of CF therapy on the gut microbiome remain to be explored.

Traditional Chinese medicines therapy is regarded as an important adjuvant approach in treatment of EC in China [2]. *Andrographis paniculata* (Burm. f.) Nees (AP) is a medicinal herb commonly used in China and south/southeast Asia [22]. Our previous studies have demonstrated the anti-tumor and anti-metastatic efficacies of AP water extract (APW), CF therapy, and their combined use in multiple EC xenograft-bearing mouse models [23-25]. However, it remains unclear whether these treatments affect the microbiome of the host. Besides, growing evidence has demonstrated that the gut microbiota can modulate the efficacy of anti-cancer drugs [26]. Therefore, we are also interested to examine if the observed anti-EC efficacy of AP is related to the gut microbiota.

Hence, in this study, we characterised the gut (stool) and esophageal microbiome in healthy and ESCC xenograft-bearing mice using high-throughput sequencing of the 16S rRNA gene. Independent and combined effects of CF therapy and AP on the gut and esophageal microbiome of xenograft-bearing mice were also elucidated. We further examined the possible functional roles of the gut microbiota in the development and metastasis of EC, as well as in the

anti-EC efficacy of AP in fecal microbiota transplantation (FMT) experiments with antibiotic-induced microbiota-depleted mice. Here, we hypothesised that (1) intraperitoneal xenograft of ESCC cells would have distinct effects on the gut and esophageal microbiome, and (2) CF therapy, AP or their combined use would alter the gut and/or esophageal microbiome. We also anticipated that (1) FMT of stool from healthy mice would reduce the development and metastasis of EC in antibiotic-induced microbiota-depleted mice, and that (2) depletion of the commensal gut microbiota would reduce the anti-EC efficacy of AP.

Materials and methods

Experimental mice

Male BALB/c nude mice (4-6 weeks old) were provided by Laboratory Animal Services Centre of The Chinese University of Hong Kong. The mice were bred and maintained in specific-pathogen free conditions with a 12-hr light/dark cycle and fed with a radiation-sterilized chow diet and autoclaved drinking water *ad libitum*. Each cage contained 3-5 mice. All experiments described in the present study were approved by the Animal Experimentation Ethics Committee of The Chinese University of Hong Kong (Ref. No. 19-131-MIS).

Cell line and reagents

Human esophageal squamous cell carcinoma (ESCC) EC-109 cells were purchased from Cell Bank of Type Culture Collection of Chinese Academy of Sciences (Beijing, China). The cells were cultured as in our previous study [24]. Cell culture medium and reagents were purchased from Life Technologies (Thermo Fisher Scientific, Waltham, MA, USA). Chemotherapeutics cisplatin and 5-fluorouracil (5-FU), and antibiotics ampicillin, neomycin, metronidazole, and vancomycin were purchased from Sigma (Sigma-Aldrich, St. Louis, MO, USA).

Herbal materials

Dried powder of AP water extract (APW) was provided by PuraPharm (Nanning) Pharmaceuticals Co. Ltd. (Batch number: CKL-20181011-Rf(H$_2$O)-). Chemical markers of APW were determined by using ultra performance liquid chromatography as follows. Dried APW sample
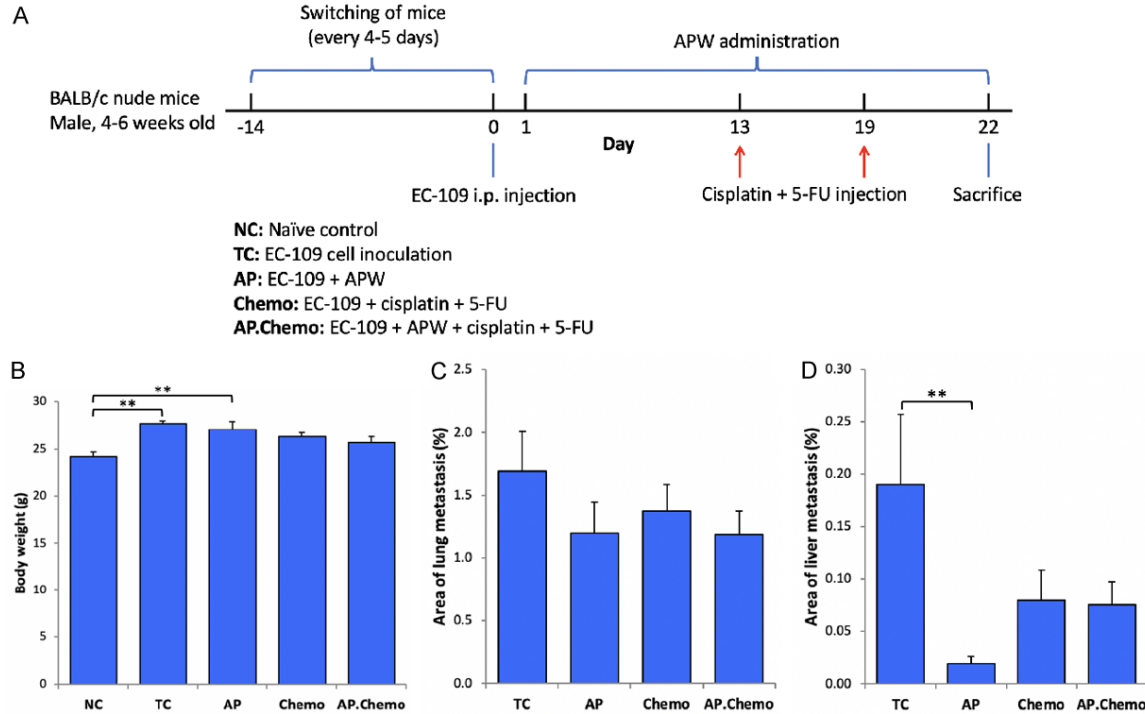
Figure 1. Cisplatin plus 5-fluorouracil (5-FU), *Andrographis paniculata* water extract (APW) and their combined use attenuate metastasis in intraperitoneal EC-109 xenograft-bearing mice. (A) Experimental design of the microbiome study. Effects of different treatments on the body weight of mice (B), and metastasis in lungs (C) and livers (D) as assessed by histology. Data represent means + SEM combined from two independent experiments (*n* = 8-14); analyzed by one-way ANOVA followed by *post-hoc* Tukey's multiple comparison test, **P < 0.01.

was dissolved in methanol, filtered through a 0.2 µm filter and then analyzed with an Agilent 1290 ultra high performance liquid chromatography system (CA, USA). The column used was Agilent ZORBAX Eclipse Plus C18 RRHD, 2.1 × 150 mm, 1.8 µm, accompanied with a guard column (Agilent ZORBAX Eclipse Plus C18 UHPLC Guard, 2.1 × 5 mm, 1.8 µm). Chromatographic separation was conducted at 40°C under gradient conditions at a flow rate of 0.5 mL/min. The LC profile is as follows: Mobile phase: (A) 0.1% formic acid in deionized water and (B) 0.1% formic acid in acetonitrile; Gradient: 0-2 min, 5% B; 2-17 min, 5-40% B; 17-18 min, 40-44% B; 18-21 min, 44% B; 21-25 min, 44-54% B; 25-27min 54-100% B. The column was flushed with 100% B for 3 min and re-equilibrated for another 4 min after each injection. The injection volume was 5 µL. APW powder was dissolved in distilled water before administration to experimental mice.

Intraperitoneal esophageal tumor xenograft-bearing mouse model

Male BALB/c nude mice were randomly switched among cages every 4-5 days for two weeks before start of the experiment to homogenize the gut microbiota of the cohort [27]. On day 0, four-fifths of mice were inoculated with 5 × 10⁶ EC-109 cells in 200 µl phosphate-buffered saline (PBS) intraperitoneally, with the remaining mice acting as naïve controls (NC). On day 1, tumor-inoculated mice were randomized into four groups: 1) tumor control (TC), 2) 1600 mg/kg APW alone (AP), 3) combination of 3.0 mg/kg cisplatin and 85.0 mg/kg 5-FU (Chemo), and 4) combination of 1600 mg/kg APW, 3.0 mg/kg cisplatin and 85.0 mg/kg 5-FU (AP.Chemo) (**Figure 1A**). Mice from each group (*n* = 7-9) were housed in two cages to reduce the cage effect. The dosage of APW (1600 mg/kg) used here was previously shown to be effective in inhibiting metastasis in human esophageal xenograft-bearing mice without obvious toxicity [23, 24]. APW was orally administered daily starting from day 1 for 21 days. On days 13 and 19, cisplatin and 5-FU were dissolved in saline and injected intraperitoneally into the mice of respective groups. In the morning of day 22, stool samples were collected from the mice, which were then anesthetized, weighed and sacrificed by cervical dislocation. Whole

esophagus, liver and lung were excised from the mice for microbiome and histological studies, respectively. Stool and esophageal samples were frozen immediately in liquid nitrogen and then stored at -80°C until DNA extraction. Liver and lung samples were fixed in 10% buffered formalin. The whole set of experiment was performed twice.

An additional set of stool samples was collected on day 22 from group TC and NC mice for fecal microbiota transplantation (FMT) experiments. For each group, two samples, each containing vortex-homogenized fecal pellets from the same 3-4 mice co-housed in a single cage and 4 mL autoclaved PBS/10% glycerol, were prepared and stored at -80°C until FMT.

Antibiotic treatment and FMT experiments

Male BALB/c nude mice were administered *ad libitum* a cocktail of antibiotics containing 0.2 g/L ampicillin, 0.2 g/L neomycin, 0.2 g/L metronidazole, and 0.1 g/L vancomycin in drinking water for two weeks before the start of the experiment to deplete the commensal gut microbiota of the cohort (**Figure 2A**) [28]. Antibiotic-containing water was freshly prepared every 3-4 days. On day 0, all mice were inoculated with 5×10^6 EC-109 cells in 200 µl PBS intraperitoneally. On day 1, the mice were randomized into six groups (*n* = 7-9 per group): 1) tumor control (TC), 2) FMT with stool of healthy mice (TCH), 3) FMT with stool of EC mice (TCE), 4) 1600 mg/kg APW alone (A), 5) 1600 mg/kg APW and FMT with stool of healthy mice (AH), and 6) 1600 mg/kg APW and FMT with stool of EC mice (AE) (**Figure 2A**). APW was orally administered daily starting from day 1 for 21 days. Frozen stool samples of healthy (NC group) and EC (TC group) mice from the previous experiment were thawed in a 37°C water bath, filtered through a Falcon 40 µm cell strainer (Corning, NY, USA), and gavaged to mice (200 µl each) on days 8 and 14. On day 22, the mice were anesthetized, weighed and sacrificed by cervical dislocation. Livers and lungs were excised from the mice and fixed in 10% buffered formalin for histological assessment. Tumor nodules in peritoneal cavity were collected, counted and weighed. The whole set of experiment was performed twice.

Histological assessment

Liver and lung samples of mice were embedded in paraffin and sectioned longitudinally at 5 µm thickness using a Thermo Scientific Shandon Finesse 325 manual microtome (Thermo Fisher Scientific, Waltham, MA, USA). Two levels of section 100 µm apart were obtained for each liver tissue blocks whereas one level of section was obtained for the lung samples. The sections were collected onto gelatin-coated slides, stained with hematoxylin & eosin for liver samples and with cytokeratin 8 for lung samples, and then photographed under an Olympus IX71 inverted research microscope (Japan) equipped with a Nikon DS-Fi3 microscope camera (Japan). The area of tumor in each slide was measured using ImageJ [29]. The degree of metastasis in each sample was evaluated by dividing the total area of tumor by the total area of organ in the slides assessed. A total of eight random microscopic fields were assessed blindly by 3-4 individuals for each sample.

Microbial DNA extraction and sequencing

Microbial DNA was extracted from about 100 mg of stool and whole esophagus of 37 mice from one out of two independent experiments using QIAamp Fast DNA Stool Mini Kit (QIAGEN, Valencia, CA, USA) following the manufacturer's instructions. For esophagus, samples were cut into tiny pieces in InhibitEX Buffer before incubation at 95°C. Extracted DNA was quantified using Invitrogen Quant-iT PicoGreen dsDNA Assay Kit (Thermo Fisher Scientific, Waltham, MA, USA). The V4 region of 16S rRNA genes was amplified with PCR using universal primers 515F (5'-GTGCCAGCMGCCGCGGTAA-3') and 806R (5'-GGACTACHVGGGTWTCTAAT-3') and Herculase II fusion DNA polymerase (Agilent Technologies, Santa Clara, CA, USA) [30]. The quality and quantity of PCR libraries were checked using an Agilent 2100 Bioanalyzer (Agilent Technologies, Santa Clara, CA, USA) and quantitative PCR according to the Illumina quantification guide, respectively. Sequencing was commercially performed by Macrogen (Seoul, Korea) on an Illumina MiSeq platform (Illumina, San Diego, CA, USA) following the 2 × 300 bp paired-end sequencing protocol. The sequencing data are available on NCBI Sequence Read Archive under BioProject accession PRJNA628535.

16S rRNA gene sequence analysis

Microbiome bioinformatics were performed with QIIME2 2020.2 [31]. Primers were first
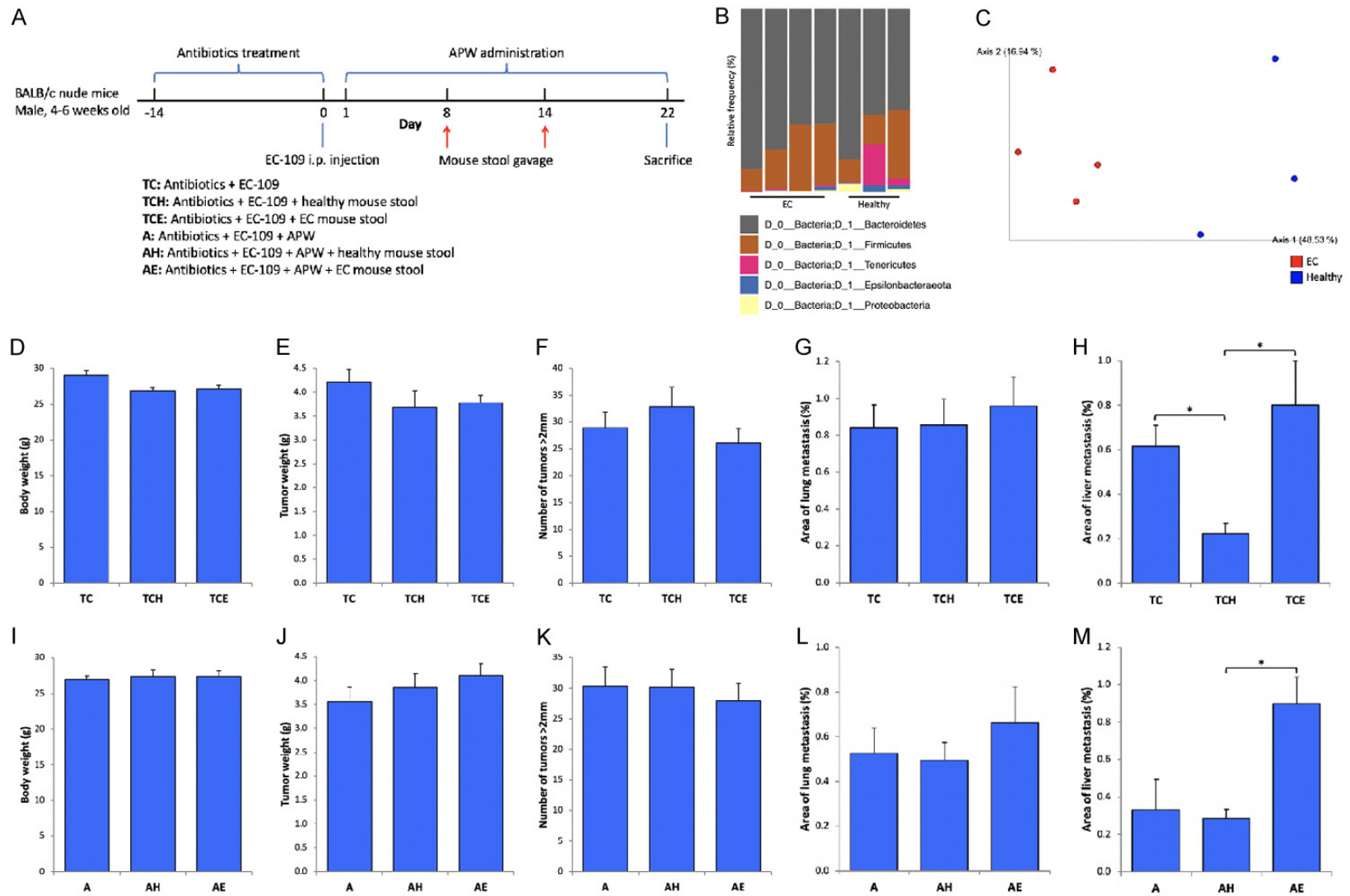
Figure 2. The commensal gut microbiota plays a role in EC metastasis and the anti-metastatic efficacy of AP. (A) Design of the fecal microbiota transplantation (FMT) experiment. Phylum-level bar chart (B) and PCoA plot (C) of the healthy and EC donor stools used in FMT (healthy vs EC, PERMANOVA pseudo-F = 3.95, P = 0.032). Effects of FMT on the body weight of mouse (D, I), tumor weight (E, J), number of tumors > 2 mm (F, K), and metastasis in lung (G, L) and liver (H, M) as assessed by histology. Data represent means + SEM combined from two independent experiments, n = 8-15 (D-F, I-K), 6-13 (G, H), and 4-10 (L, M); analyzed by one-way ANOVA followed by *post-hoc* Tukey's multiple comparison test, *P < 0.05.

removed from demultiplexed raw sequence data using the q2-cutadapt plugin [32]. No insertions or deletions of bases were allowed when matching primers, and reads with no primer found were discarded. Paired-end reads were then joined using q2-vsearch [33], quality-filtered using q2-quality-filter, and denoised with Deblur using q2-deblur [34]. Taxonomy was assigned to amplicon sequence variants (ASVs) using a pre-trained Naïve Bayes classifier using q2-feature-classifier against the SILVA 132 99% operational taxonomic units (OTUs) from the 515F/806R sequence dataset [35, 36]. ASVs with a total read count < 10 or present in only one sample were removed using q2-feature-table. Mitochondrial, chloroplast and phylum-unclassified reads were also filtered out using q2-taxa. All ASVs were aligned with mafft and used to construct a phylogenetic tree with fasttree2 using q2-phylogeny, with the align-to-tree-mafft-fasttree pipeline [37, 38]. Alpha and beta diversity metrics as well as principal coordinate analysis (PCoA) plots were generated using the q2-diversity plugin with the core-metrics-phylogenetic pipeline after samples were rarefied to the smallest number of sequences. Alpha diversity metrics computed included the number of observed OTUs, Faith's phylogenetic diversity, Pielou's evenness, and Shannon's diversity, whereas Bray-Curtis dissimilarity was computed for beta diversity estimation. Alpha rarefaction curves were also generated using the same plugin. Associations between categorical metadata and alpha diversity metrics and sample composition were tested using q2-diversity with the alpha-group-significance and beta-group-significance functions, respectively. Pairwise comparisons of differentially abundant taxa at different taxonomic levels among experimental groups were performed using analysis of composition of microbiomes (ANCOM), which accounts for compositionality using log-ratios [39]. Venn diagrams of shared ASVs were drawn using jvenn [40].

Prediction of functional potential

Microbial functional potential was predicted using PICRUSt v1.1.1 on the online Galaxy server (http://galaxy.morganlangille.com/) [41]. PICRUSt-compatible OTU tables were prepared by filtering *de novo* chimeras from quality-filtered joined reads, followed by closed-reference OTU picking at 97% identity against the Greengenes 13_5 97% OTUs sequence dataset [42], both using the q2-vsearch plugin of QIIME2 2020.2. Pairwise comparisons of differentially abundant Kyoto Encyclopedia of Genes and Genomes (KEGG) pathways among treatment groups were performed on the predicted metagenomes using STAMP v2.1.3 [43]. The accuracy of prediction was quantified with the nearest sequenced taxon index.

Statistical analysis

All measurements are shown as mean + SEM and statistically compared among groups using one-way analysis of variance (ANOVA) followed by *post-hoc* Tukey's multiple comparison tests. Differences in alpha diversity among groups were tested using Kruskal-Wallis tests with *P* values corrected by the Benjamini-Hochberg method, whereas differences in beta diversity among groups in PCoA were tested using permutational multivariate analysis of variance (PERMANOVA) with 999 permutations in QIIME2. Pairwise differences in predicted KEGG pathways between groups were tested using Welch's *t*-tests with *P* values corrected by the Storey's FDR multiple test correction method in STAMP. Differences were considered to be statistically significant when *P* < 0.05.

Results

The gut and esophageal microbiome in nude mice are distinct

Athymic nude mice remain one of the most widely used animal models in cancer research, particularly as a tool for preclinical testing of drugs [44]. In this study, we characterised the gut and esophageal microbiome in a cohort of BALB/c nude mice (*n* = 37) via 16S rRNA gene sequencing. Mice were either untreated (*n* = 7), xenografted with human EC-109 cells (*n* = 7), treated with commonly used chemotherapeutics cisplatin and 5-FU (*n* = 8), treated with the medicinal herb *A. paniculata* water extract (*n* = 9), or received a combined treatment (chemotherapeutics plus herbal extract) (*n* = 6) (**Figure 1A**). Stool and esophagus samples were collected from each mouse in the cohort. As a result, a total of 74 samples (37 stool and 37 esophagus samples) were sequenced and analyzed in this study.

Rarefaction curves of all 74 samples reached plateaus at 33,000 reads per sample, showing that the depth of sequencing was high enough to capture the full diversity of the microbiome (**Figure 3A**). Principal coordinate analysis (PCoA) based on Bray-Curtis dissimilarity of all samples revealed a significant difference in the overall structure of the gut and esophageal microbiome (PERMANOVA, *P* = 0.001) (**Figure 3B**). The gut microbiome was dominated by the bacterial phyla *Bacteroidetes* (67.9% on average) and *Firmicutes* (27.8%) (**Figure 4A**), and the families *Muribaculaceae* (30.0%), *Bacteroidaceae* (17.7%), *Rikenellaceae* (17.0%), and *Lachnospiraceae* (16.6%) (**Figure 4B**). By contrast, the esophageal microbiome was dominated by the phyla *Firmicutes* (79.8%) and *Proteobacteria* (15.1%) (**Figure 5A**), and the families *Lactobacillaceae* (70.4%) and *Pasteurellaceae* (13.9%) (**Figure 5B**).

We then focused on the comparison of the gut and esophageal microbiome in naïve control and tumor control mice. In naïve control mice, the number of observed operational taxonomic units (OTUs) and evenness were significantly higher in the stool than the esophagus samples ($P < 0.05$) (**Figures 4C-F, 5C-F**). Analysis of composition of microbiomes (ANCOM) revealed significant enrichments of the order *Bacteroidales* (W = 28) and the families *Bacteroidaceae* (W = 46) and *Tannerellaceae* (W = 43) in the stool samples ($P < 0.05$) (**Figure 3C**). By contrast, the families *Lactobacillaceae* (W = 56), *Pasteurellaceae* (W = 56), *Pseudomonadaceae* (W = 47), *Moraxellaceae* (W = 42), and *Streptococcaceae* (W = 42) were enriched in the esophagus samples ($P < 0.05$). While at the amplicon sequence variant (ASV) level, a taxon belonging to *Lactobacillus murinus* (W = 413) and another belonging to the family *Pasteurellaceae* (W = 413) were enriched in the esophagus samples ($P < 0.05$). In tumor control mice, the number of observed OTUs, Faith's phylogenetic diversity, evenness, and Shannon diversity were all significantly higher in the stool than the esophagus samples ($P < 0.01$) (**Figures 4C-F, 5C-F**). ANCOM revealed significant enrichments of the phyla *Bacteroidetes* (W = 5) and *Patescibacteria* (W = 4) in the stool samples, and enrichments of *Actinobacteria* (W = 5), *Firmicutes* (W = 5) and *Proteobacteria* (W = 5) in the esophagus samples ($P < 0.05$) (**Figure 3D**). While at the ASV level, four taxa belonging
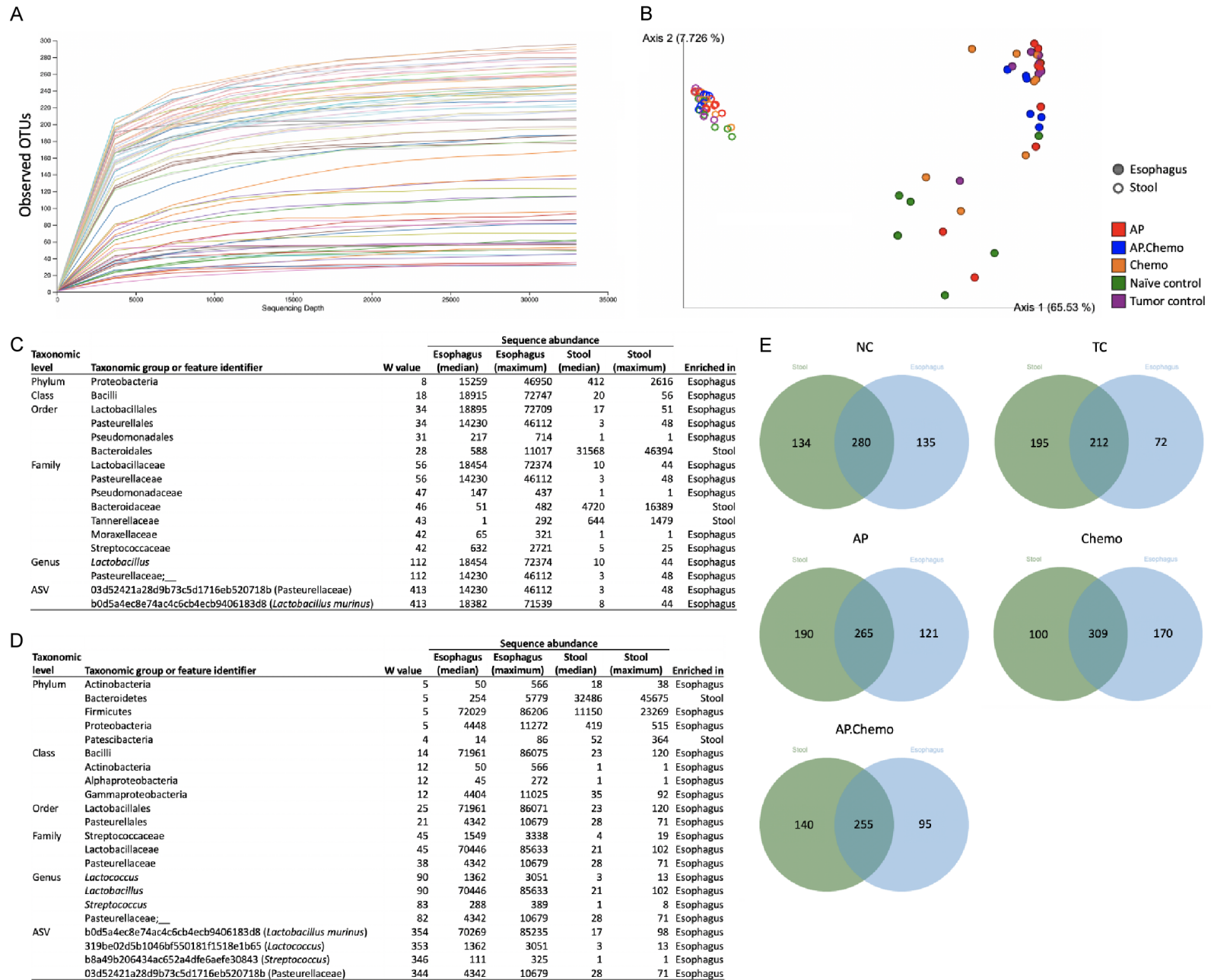
to *Lactobacillus murinus* (W = 354), the genera *Lactococcus* (W = 353) and *Streptococcus* (W = 346), and the family *Pasteurellaceae* (W = 344) were enriched in the esophagus samples ($P < 0.05$). Besides, we attempted to examine the potential correlation of the dominant phyla (*Firmicutes*, *Bacteroidetes* and *Proteobacteria*) between the gut and esophageal microbiome in naïve control and tumor control mice; however, no significant correlation was found (Spearman's correlation test, $P > 0.05$).

Intraperitoneal xenograft of EC-109 cells alters the gut and esophageal microbiome

We then examined the effects of intraperitoneal inoculation of EC-109 cells on the gut and esophageal microbiome in BALB/c nude mice by comparing results of tumor control mice with naïve control mice. EC-109 inoculation did not significantly affect the bacterial richness, evenness and Shannon diversity of the gut microbiome ($P > 0.05$) (**Figure 4C-F**). However, PCoA revealed a significantly altered gut microbiome structure in tumor control mice (PERMANOVA, $P = 0.005$) (**Figure 4G**). ANCOM also revealed a significant depletion of the order *Pasteurellales* in the gut microbiome of tumor control mice (W = 3, $P < 0.05$) (**Figure 4H**). A previous study has demonstrated an extensive transmission of microbes along the gastrointestinal tract of healthy persons, and that the level of transmission is increased in colorectal cancer (CRC) patients [45]. Here, a higher proportion of esophageal ASVs was also found in the stool samples of tumor control mice (74.6%) as compared to that in naïve control mice (67.5%) (**Figure 3E**). Besides, the ratio of Firmicutes to Bacteroidetes (F/B ratio) of the gut microbiome has been regarded as an indicator of health status [46]. However, in this study, no significant difference in the F/B ratio of the gut microbiome was observed between tumor control and naïve control mice, and in fact among all experimental groups ($P > 0.05$) (**Figure 4I**). Finally, we attempted to predict the functional potential of the gut microbiome from the 16S rRNA sequences using PICRUSt [41]. However, a high average nearest sequenced taxon index of 0.226 indicates a low prediction accuracy and precluded further analysis [41].

In the case of esophageal microbiome, the bacterial richness, evenness and Shannon diversi-
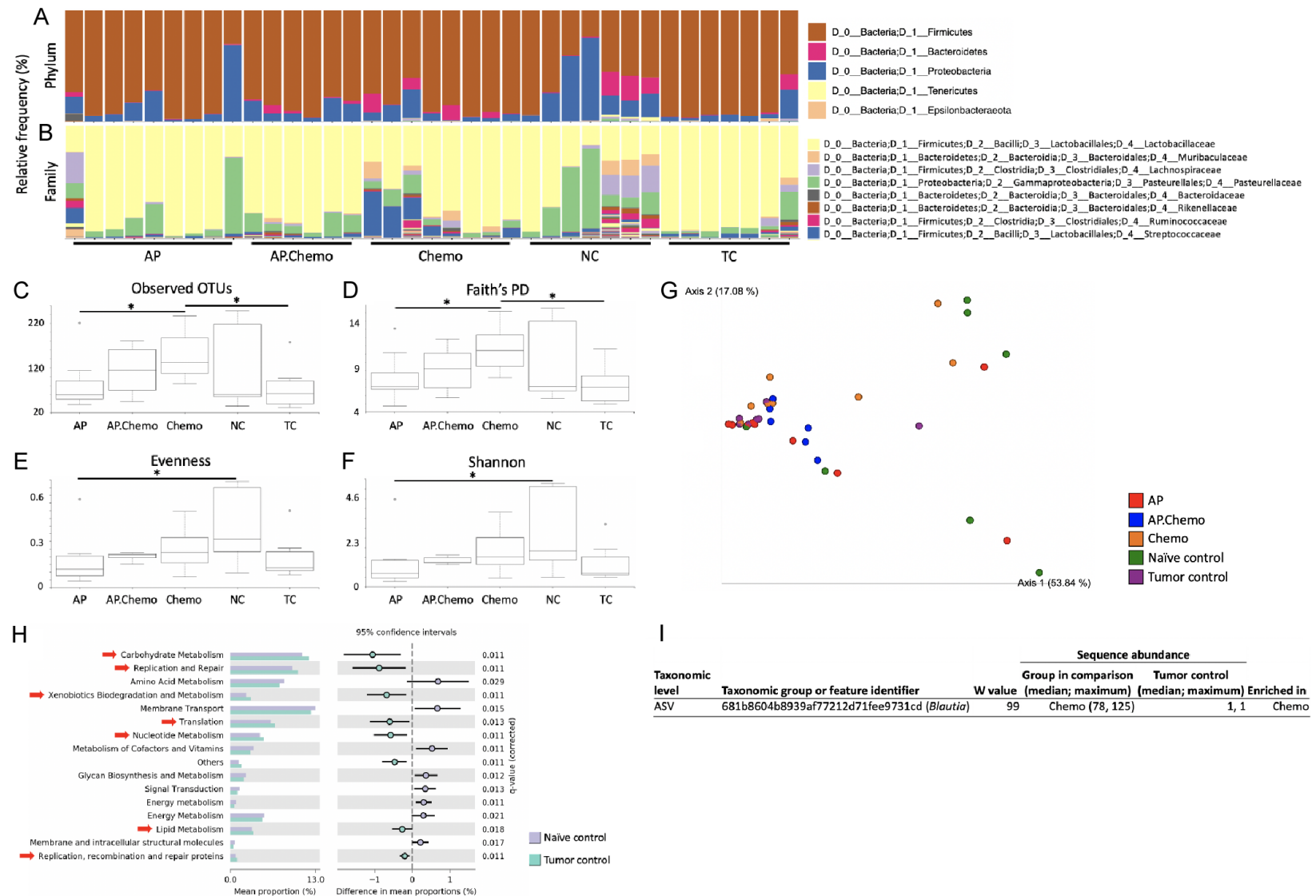
Interplay between gut microbiota and esophageal cancer

A (rarefaction curve: Observed OTUs vs Sequencing Depth)

B (PCoA plot: Axis 1 (65.53 %) vs Axis 2 (7.726 %))

Legend: Esophagus (filled), Stool (open); AP, AP.Chemo, Chemo, Naïve control, Tumor control

C

| Taxonomic level | Taxonomic group or feature identifier | W value | Sequence abundance | | | | Enriched in |
			Esophagus (median)	Esophagus (maximum)	Stool (median)	Stool (maximum)	
Phylum	Proteobacteria	8	15259	46950	412	2616	Esophagus
Class	Bacilli	18	18915	72747	20	56	Esophagus
Order	Lactobacillales	34	18895	72709	17	51	Esophagus
	Pasteurellales	34	14230	46112	3	48	Esophagus
	Pseudomonadales	31	217	714	1	1	Esophagus
	Bacteroidales	28	588	11017	31568	46394	Stool
Family	Lactobacillaceae	56	18454	72374	10	44	Esophagus
	Pasteurellaceae	56	14230	46112	3	48	Esophagus
	Pseudomonadaceae	47	147	437	1	1	Esophagus
	Bacteroidaceae	46	51	482	4720	16389	Stool
	Tannerellaceae	43	1	292	644	1479	Stool
	Moraxellaceae	42	65	321	1	1	Esophagus
	Streptococcaceae	42	632	2721	5	25	Esophagus
Genus	*Lactobacillus*	112	18454	72374	10	44	Esophagus
	Pasteurellaceae;___	112	14230	46112	3	48	Esophagus
ASV	03d52421a28d9b73c5d1716eb520718b (Pasteurellaceae)	413	14230	46112	3	48	Esophagus
	b0d5a4ec8e74ac4c6cb4ecb9406183d8 (*Lactobacillus murinus*)	413	18382	71539	8	44	Esophagus

D

| Taxonomic level | Taxonomic group or feature identifier | W value | Sequence abundance | | | | Enriched in |
			Esophagus (median)	Esophagus (maximum)	Stool (median)	Stool (maximum)	
Phylum	Actinobacteria	5	50	566	18	38	Esophagus
	Bacteroidetes	5	254	5779	32486	45675	Stool
	Firmicutes	5	72029	86206	11150	23269	Esophagus
	Proteobacteria	5	4448	11272	419	515	Esophagus
	Patescibacteria	4	14	86	52	364	Stool
Class	Bacilli	14	71961	86075	23	120	Esophagus
	Actinobacteria	12	50	566	1	1	Esophagus
	Alphaproteobacteria	12	45	272	1	1	Esophagus
	Gammaproteobacteria	12	4404	11025	35	92	Esophagus
Order	Lactobacillales	25	71961	86071	23	120	Esophagus
	Pasteurellales	21	4342	10679	28	71	Esophagus
Family	Streptococcaceae	45	1549	3338	4	19	Esophagus
	Lactobacillaceae	45	70446	85633	21	102	Esophagus
	Pasteurellaceae	38	4342	10679	28	71	Esophagus
Genus	*Lactococcus*	90	1362	3051	3	13	Esophagus
	Lactobacillus	90	70446	85633	21	102	Esophagus
	Streptococcus	83	288	389	1	8	Esophagus
	Pasteurellaceae;___	82	4342	10679	28	71	Esophagus
ASV	b0d5a4ec8e74ac4c6cb4ecb9406183d8 (*Lactobacillus murinus*)	354	70269	85235	17	98	Esophagus
	319be02d5b1046bf550181f1518e1b65 (*Lactococcus*)	353	1362	3051	3	13	Esophagus
	b8a49b206434ac652a4dfe6aefe30843 (*Streptococcus*)	346	111	325	1	1	Esophagus
	03d52421a28d9b73c5d1716eb520718b (Pasteurellaceae)	344	4342	10679	28	71	Esophagus

E

NC: Stool 134, 280, Esophagus 135
TC: Stool 195, 212, Esophagus 72
AP: Stool 190, 265, Esophagus 121
Chemo: Stool 100, 309, Esophagus 170
AP.Chemo: Stool 140, 255, Esophagus 95

Figure 3. The gut and esophageal microbiome in nude mice are distinct. (A) Rarefaction curves of the number of observed operational taxonomic units (OTUs) at 100% similarity for all 74 samples in this study. (B) Principal coordinate analysis (PCoA) plot based on Bray-Curtis dissimilarity of 37 stool and 37 esophagus samples (stool vs esophagus, PERMANOVA pseudo-F = 127.36, P = 0.001). Differentially abundant taxa (P < 0.05) at all taxonomic levels between the gut and esophageal microbiome in naïve control (C) and tumor control mice (D) as detected by ANCOM. For each amplicon sequence variant (ASV), identity at the lowest possible taxonomic level is given in brackets; W value equals to the number of ANCOM sub-hypotheses that have passed for a given taxon. (E) Venn diagrams of shared and unique ASVs between the stool (green) and esophagus (blue) samples in each group.
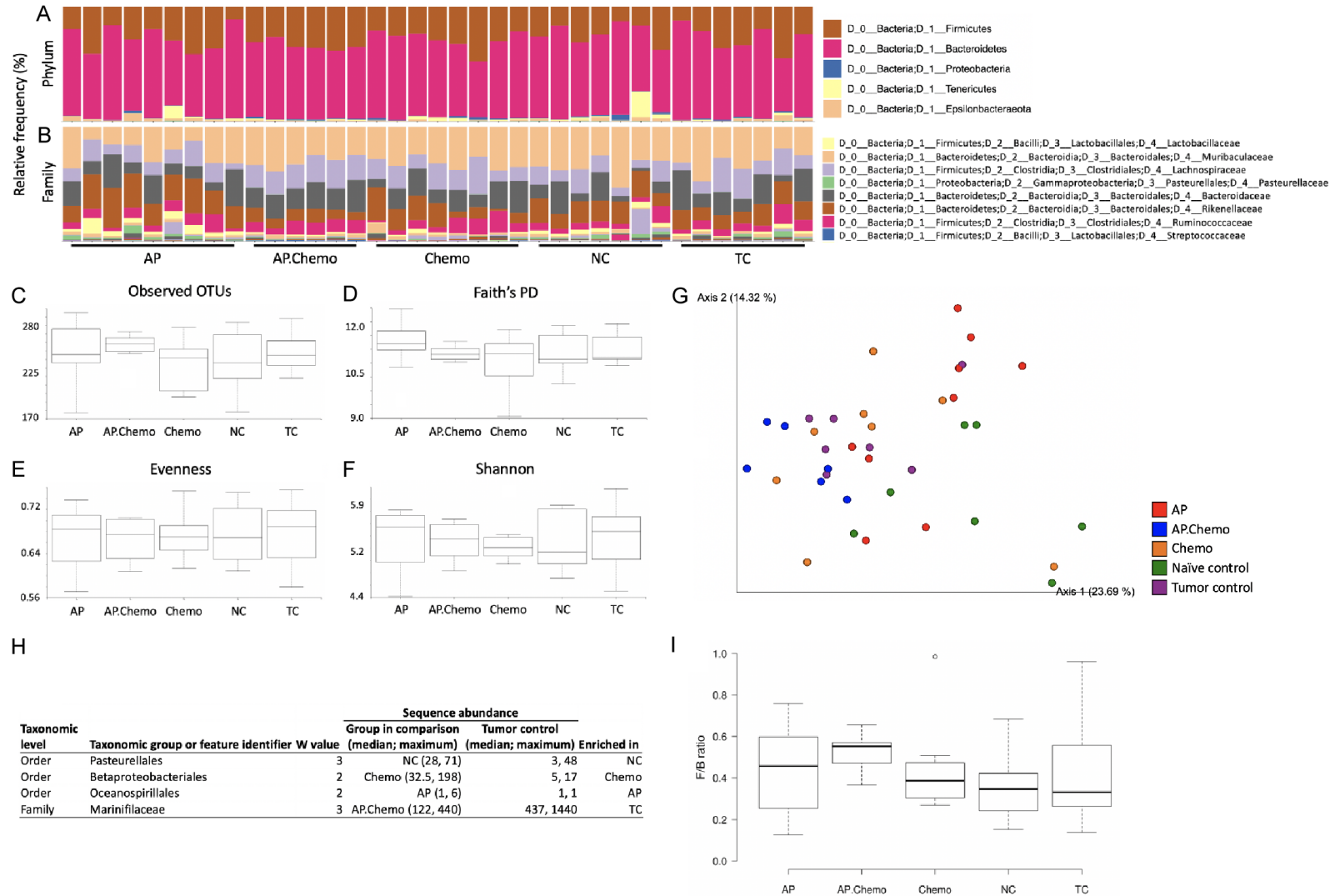
Figure 4. Effects of intraperitoneal EC-109 xenograft, cisplatin plus 5-FU combination chemotherapy (CF therapy), AP water extract, and CF therapy plus AP combined treatment on the murine gut microbiome. Taxonomic composition of the gut microbiome at the phylum (A) and family level (B) for each sample. Comparison of alpha diversity among groups based on the number of observed OTUs (C), Faith's phylogenetic diversity (D), evenness (E), and Shannon diversity (F). (G) PCoA plot of all 37 stool samples (naïve control vs tumor control, PERMANOVA pseudo-F = 3.17, P = 0.005; AP vs tumor control, PERMANOVA pseudo-F = 1.95, P = 0.045). (H) Differentially abundant taxa (P < 0.05) at all taxonomic levels in the gut microbiome among all groups as detected by ANCOM. (I) Ratio of Firmicutes to Bacteroidetes.

Figure 5. Effects of intraperitoneal EC-109 xenograft, CF therapy, AP water extract, and CF therapy plus AP combined treatment on the murine esophageal microbiome. Taxonomic composition of the esophageal microbiome at the phylum (A) and family level (B) for each sample. Comparison of alpha diversity among groups based on the number of observed OTUs (C), Faith's phylogenetic diversity (D), evenness (E), and Shannon diversity (F). Statistical difference among groups was tested using Kruskal-Wallis tests with P values corrected by the Benjamini-Hochberg method, *P < 0.05. (G) PCoA plot of all 37 esophagus samples (naïve control vs tumor control, PERMANOVA pseudo-F = 5.34, P = 0.007). (H) Differentially abundant level 2 KEGG pathways in the esophageal microbiome between naïve control and tumor control mice. Statistical difference between groups was tested using Welch's t-tests with P values corrected by the Storey's FDR multiple test correction method. Only significantly different (q < 0.05) pathways with an effect size of > 0.2% difference in mean proportions are shown; pathways enriched in tumor control are indicated with a red arrow. (I) The only differentially abundant taxon (P < 0.05) across all taxonomic levels in the esophageal microbiome among groups as detected by ANCOM. Identity of the ASV at the lowest possible taxonomic level is given in brackets; W value equals to the number of ANCOM sub-hypotheses that have passed.

ty tended to be lower in tumor control mice, although the effects were not statistically significant (**Figure 5C-F**). PCoA revealed a significantly altered esophageal microbiome structure in tumor control mice (PERMANOVA, P = 0.007) (**Figure 5G**). However, ANCOM did not reveal any significant enrichment/depletion of taxa in the esophageal microbiome of tumor control mice. We then predicted the functional potential of the esophageal microbiome using PICRUSt. An average nearest sequenced taxon index of 0.047 indicates a high prediction accuracy [41]. Significantly differentially abundant (q < 0.05) Kyoto Encyclopedia of Genes and Genomes (KEGG) pathways were only detected between tumor control and naïve control mice. Level 2 KEGG pathways related to carbohydrate metabolism, replication and repair, xenobiotics biodegradation and metabolism, translation, nucleotide metabolism, lipid metabolism, and replication, recombination and repair proteins were significantly enriched in the esophageal microbiome of tumor control mice (P < 0.05) (**Figure 5H**).

The commensal gut microbiota of healthy mice protects against liver metastasis of EC

To examine the possible functional roles of the gut microbiota in the development and metastasis of EC, we depleted the commensal gut microbiota of BALB/c nude mice (n = 21 or 23, in two independent experiments) by adding in their drinking water a cocktail of broad-spectrum antibiotics for 14 days before intraperitoneal inoculation of EC-109 cells, followed by two rounds of FMT of stools from either naïve control mice (healthy mice) or EC-109 xenograft-bearing mice (EC mice) on the 8th and 14th days (**Figure 2A**). Each of the three experimental groups contained 7 to 8 mice in each independent experiment.

The taxonomic composition of individual donor stools is shown in a phylum-level bar chart (**Figure 2B**). PCoA confirmed that the healthy and EC donor stools were significantly different in the overall microbiome structure (PERMANOVA, P = 0.030) (**Figure 2C**). FMT of healthy or EC mouse stools did not significantly affect the body weight of mice, total tumor weight or the number of tumors > 2 mm in size (P > 0.05) (**Figure 2D-F**), suggesting that the gut microbiota of healthy and EC mice do not promote the growth of EC tumors. Besides, FMT of healthy or EC mouse stools did not significantly affect the area of lung metastasis as assessed by histology (P > 0.05) (**Figure 2G**). However, interestingly, FMT of healthy mouse stools significantly reduced the area of liver metastasis in microbiota-depleted mice (P < 0.05) (**Figure 2H**), to an extent comparable to that in microbiota-intact tumor control mice (**Figure 1D**). By contrast, FMT of EC mouse stools did not significantly affect the area of liver metastasis, although there was a trend of increase (**Figure 2H**). Collectively, these findings suggest a T cell-independent protective role of the commensal gut microbiota and/or their metabolites of healthy mice in liver metastasis of EC.

Combination chemotherapy with cisplatin and 5-FU (CF therapy) differentially affects the gut and esophageal microbiome in EC-109 xenograft-bearing mice

We then proceeded to examine the effects of CF therapy on the gut and esophageal microbiome in EC-109 xenograft-bearing mice by comparing results of CF therapy-treated mice with tumor control mice. CF therapy did not significantly affect the body weight of mice (P > 0.05) (**Figure 1B**) but tended to reduce the area of lung and liver metastasis, albeit the effects were not statistically significant (**Figure 1C**, **1D**).

CF therapy did not significantly affect the bacterial richness, evenness and Shannon diversity of the gut microbiome ($P > 0.05$) (**Figure 4C-F**). PCoA revealed that CF therapy did not significantly alter the structure of the gut microbiome either (PERMANOVA, $P = 0.355$) (**Figure 4G**). However, ANCOM revealed a significant enrichment of the order *Betaproteobacteriales* in the gut microbiome of CF therapy-treated mice (W = 2, $P < 0.05$) (**Figure 4H**).

In the case of esophageal microbiome, CF therapy significantly increased the bacterial richness ($P < 0.05$) but did not affect evenness and Shannon diversity (**Figure 5C-F**). A higher proportion of stool ASVs was found in the esophagus samples of CF therapy-treated mice (75.6%) as compared to that in tumor control mice (52.1%) (**Figure 3E**). Besides, PCoA revealed that CF therapy did not significantly alter the structure of the esophageal microbiome (PERMANOVA, $P = 0.142$) (**Figure 5G**). However, ANCOM revealed a significant enrichment of an ASV belonging to the genus *Blautia* in the esophageal microbiome of CF therapy-treated mice (W = 99, $P < 0.05$) (**Figure 5I**).

Treatment with AP alone or combined with CF therapy only affects the microbiome of the gut, but not the esophagus, in EC-109 xenograft-bearing mice

We continued to examine the effects of AP and its combined use with CF therapy on the gut and esophageal microbiome in EC-109 xenograft-bearing mice by comparing results of mice treated with AP alone or together with CF therapy with tumor control mice. Ultra performance liquid chromatography analysis revealed that the main chemical component of AP was andrographolide (**Figure 6**). AP or its combined use with CF therapy did not significantly affect the body weight of mice ($P > 0.05$) (**Figure 1B**). Although statistically insignificant, both treatments tended to reduce the area of lung metastasis as assessed by histology (**Figure 1C**). Besides, AP administration significantly reduced the area of liver metastasis ($P < 0.01$), whereas its combined use with CF therapy tended to reduce it (**Figure 1D**).

AP and its combined use with CF therapy did not significantly alter the bacterial richness, evenness and Shannon diversity of the gut microbiome ($P > 0.05$) (**Figure 4C-F**). PCoA revealed a significantly altered gut microbiome structure in AP-treated mice (PERMANOVA, $P = 0.045$) (**Figure 4G**). However, combined treatment with AP and CF therapy did not significantly alter the structure of the gut microbiome (PERMANOVA, $P = 0.053$). ANCOM revealed a significant enrichment of the order *Oceanospirillales* in the gut microbiome of AP-treated mice (W = 2, $P < 0.05$) (**Figure 4H**), and depletion of the family *Marinifilaceae* in the gut microbiome of mice receiving a combined treatment (W = 3, $P < 0.05$) (**Figure 4H**).

There was no significant difference in the bacterial richness, evenness and Shannon diversity of the esophageal microbiome between AP-treated mice and tumor control mice ($P > 0.05$) (**Figure 5C-F**). Combined treatment with AP and CF therapy also insignificantly affected the bacterial richness, evenness and Shannon diversity of the esophageal microbiome, although there was a trend towards higher values in the treatment group (**Figure 5C-F**). PCoA revealed that AP, either combined or not combined with CF therapy, did not significantly alter the structure of the esophageal microbiome (PERMANOVA, AP: $P = 0.382$, AP.Chemo: $P = 0.771$) (**Figure 5G**). Besides, no significant enrichment/depletion of any taxa was detected by ANCOM in the esophageal microbiome of mice treated with AP alone or together with CF therapy.

The commensal gut microbiota of mice plays a role in the anti-metastatic efficacy of AP

To examine the possible functional roles of the gut microbiota in the anti-EC efficacy of AP, we depleted the commensal gut microbiota of BALB/c nude mice ($n = 21$ or 24, in two independent experiments) by a broad-spectrum antibiotic cocktail for 14 days before intraperitoneal inoculation of EC-109 cells, followed by two rounds of FMT of stools from either healthy mice or EC mice during a 21-days treatment course with AP (**Figure 2A**). Each of the three experimental groups contained 7 to 9 mice in each independent experiment.

FMT of healthy or EC mouse stools did not significantly affect the body weight of mice or the anti-tumor efficacy of AP (**Figure 2I-K**). FMT of healthy or EC mouse stools also did not significantly affect the anti-metastatic efficacy of AP on lung metastasis (**Figure 2L**). However, the
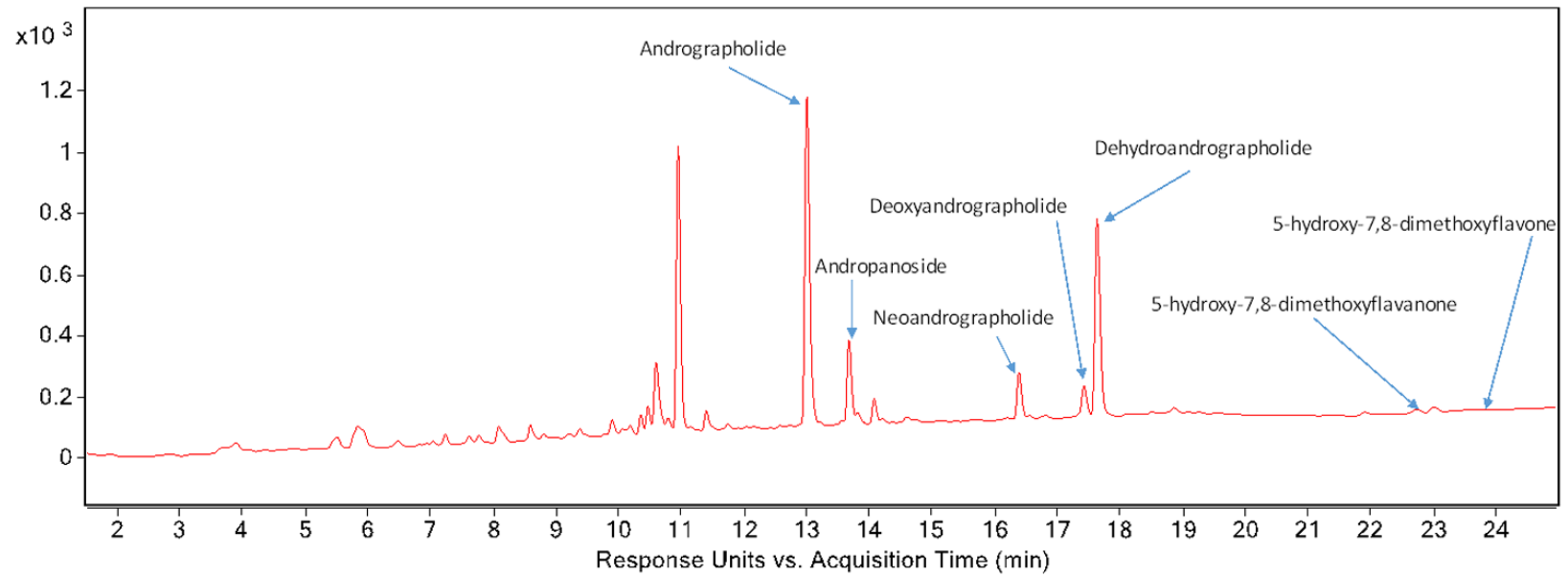
Figure 6. Ultra performance liquid chromatography profile of APW with chemical markers indicated by arrows. Detection wavelength at 226 nm.

antibiotic treatment reduced the anti-metastatic efficacy of AP on liver metastasis from 89.5% in microbiota-intact mice (**Figure 1D**) to 46.8% in microbiota-depleted mice (**Figure 2H**, **2M**). In fact, the reduced efficacy cannot be restored by FMT of healthy or EC mouse stools (**Figure 2M**). These findings suggest that the anti-metastatic efficacy of AP on liver metastasis of EC relies, at least partly, on the commensal gut microbiota.

Discussion

The gut microbiota plays important roles in cancer development [16]. Until now, there is only one study which examines the gut microbiome in EC [17]. Conducted in 8-10 weeks old female BALB/c nude mice with EC-109 cells subcutaneously injected into the flank, Zhou and colleagues show that xenograft-bearing mice and normal control mice display a different gut microbiota structure, in concordance with our results. However, a significant increase in the phylum *Bacteroidetes* and a decrease in *Firmicutes* in xenograft-bearing mice are reported in that study, which are not observed in our work. With the strain and age of mice, tumor cell line, amount of inoculum, duration of study, and the gut microbiota composition of normal control mice being the same or similar between the two studies, possible reasons for the discrepancy include the sex of mice and the route of tumor cell injection [47, 48]. Besides, we reveal a significant depletion of the order *Pasteurellales* in the gut microbiome of EC xenograft-bearing mice. Bacteria belonging to this order are mostly harmless commensals of humans [49]. In fact, a depletion of *Pasteurellales* is also reported in the gut microbiome in patients with CRC and in the oral microbiome in those with pancreatic ductal adenocarcinoma as compared to healthy subjects [50, 51]. Moreover, the F/B ratio of the gut microbiome has been regarded as an indicator of health status [46]. The F/B ratio is reported to be higher in rats with gastric cancer [52], lower in patients with primary liver cancer or lung cancer [53, 54], and unchanged in CRC patients as compared to normal controls [55]. Here, we observe no significant difference in the F/B ratio of the gut microbiome between EC xenograft-bearing and naïve control mice, suggesting that the ratio cannot be used as an indicator of EC, just like in the case of CRC.

Apart from the gut microbiome, our results showed that intraperitoneal inoculation of ESCC cells also significantly alters the structure of the esophageal microbiome in mice. Indeed, a distinct microbiota structure is also reported in the esophageal mucosa of patients with esophageal adenocarcinoma as compared with healthy subjects [12], and in the microbiota of paired tumor and non-tumor tissues from patients with ESCC [10]. Besides, xenograft-bearing mice tend to have a lower alpha diversity in the esophageal microbiome as compared with naïve control mice, in agreement with results from a previous case-control study [8]. Moreover, 16S rRNA-based functional potential prediction showed that KEGG pathways related to carbohydrate metabolism, replication and repair, xenobiotics biodegradation and metabolism, translation, nucleotide metabolism, lipid metabolism, and replication, recombination and repair proteins are significantly enriched in the esophageal microbiome of xenograft-bearing mice. Pathways related to carbohydrate metabolism, xenobiotics biodegradation and metabolism, and lipid metabolism are also enriched in the gastric microbiome of patients with gastric carcinoma as compared to those with chronic gastritis [56]. Enrichments of these metabolic pathways in general agree with the metabolic reprogramming required for cancer progression [57].

The commensal gut microbiota has been shown to promote tumorigenesis in multiple cancers, including hepatocellular carcinoma and pancreatic ductal adenocarcinoma [58, 59]. Here, via FMT experiments, we showed that the gut microbiota of healthy or EC mice does not promote growth of EC xenografts in nude mice. By contrast, we showed that FMT of healthy mouse stool significantly attenuates liver metastasis in microbiota-depleted nude mice, suggesting a T cell-independent protective role of the commensal gut microbiota and/or their metabolites of healthy mice in metastasis of EC. This finding aligns with the results of a population-based case-control study that a higher risk of EC is observed in individuals with repeated exposure to antibiotics [18]. In fact, a protective role of the commensal gut microbiota has also been reported in CRC [60], pneumococcal pneumonia [61], acute arsenic toxicity [62], and polycystic ovary syndrome [63]. Our finding provides the first piece of preliminary evidence

on the potential use of FMT as a treatment strategy to attenuate metastasis in EC. At present, FMT is recommended in the treatment of recurrent *Clostridium difficile* infection, with a clinical efficacy reaching 90% [64]. Multiple case reports and series have also revealed the potential of FMT in alleviating various cancers [65]; however, randomized controlled trials are required to delineate the validity of FMT for cancer treatment. In fact, a few clinical trials are ongoing to study the use of FMT in the context of cancer therapy [16].

Here, we showed that CF therapy does not significantly affect the alpha or beta diversity of the gut microbiome in xenograft-bearing mice. Previous studies have reported a reduced alpha diversity and/or an altered beta diversity of the gut microbiome in tumor-bearing mice treated with 5-FU or cisplatin [17, 20, 66]. Possible reasons for the discrepancies observed here include the treatment scheme and possible interactions of drugs, among others. By contrast, CF therapy significantly increases the bacterial richness of the esophageal microbiome. This, together with the fact that a higher proportion of stool ASVs is found in the esophagus samples of CF therapy-treated mice as compared with xenograft-bearing mice, suggests the presence of bacterial translocation from the gut to the esophagus [67]. Bacterial translocation is a phenomenon commonly associated with intestinal mucositis caused by chemotherapeutics [68]. Besides, we observe a significant enrichment of an ASV belonging to the genus *Blautia* in the esophageal microbiome of CF therapy-treated mice. This genus comprises 3.3% of the gut microbiome in CF therapy-treated mice; therefore, it is possible that the enriched *Blautia* in the esophageal microbiome is also a result of bacterial translocation. However, further experiments, for instance, with oral administration of fluorescently labeled bacterial strains to mice [69], are needed to confirm the presence of gut-to-esophagus translocation.

Our previous *in vitro* and *in vivo* studies have demonstrated the anti-EC efficacy of APW, especially its anti-metastatic efficacy [23-25]. Here, we showed that APW administration significantly alters the microbiota structure of the gut, but not that of the esophagus. In fact, the capability of medicinal botanicals and their compounds to modulate the gut microbiota in

cancers has been well documented [70]. However, whether the altered microbiome plays a direct role in the anti-tumor outcomes remains to be elucidated by further functional or mechanistic studies on individual bacterial taxon involved. Interestingly, we showed that treatment with broad-spectrum antibiotics reduces the anti-metastatic efficacy of AP on liver metastasis in xenograft-bearing mice by half, suggesting that the anti-metastatic efficacy of AP on liver metastasis of EC relies, at least partly, on the commensal gut microbiota. In fact, the gut microbiota has also been shown to affect the efficacy of anti-cancer drugs [26]. For instance, antibiotics treatment is reported to reduce the antitumor efficacy of 5-FU in mice [66]. The gut microbiota is in fact metabolically active, and can metabolise with its arsenal of enzymes those compounds present in traditional Chinese medicines via reactions such as hydrolysis, oxidation and reduction, among others [71]. As andrographolide, the main active component of AP, has demonstrated anti-metastatic efficacy [72], we thus postulate that its transformation by the commensal gut microbiota is required for the anti-metastatic efficacy of AP in EC. Besides, our finding has practical implications that AP should not be administered together with antibiotics for best efficacy in EC treatment. Lastly, it is noteworthy that the reduced efficacy after antibiotic treatment cannot be restored by FMT of stool from healthy mice. Although we have followed the guidelines on preparing stools for FMT in this study [73], it is still possible that the transplanted bacteria did not successfully colonise or grow in the gut of mice. However, this actually shows that it is the active gut microbiota itself, but not its metabolites, that affects the anti-metastatic efficacy of AP in EC.

In conclusion, this study has revealed for the first time an interplay between the gut microbiota and EC, and provided insights into treatment strategies for EC. Further work in immunocompetent mouse models and clinical research are needed to better understand how the gut microbiota affects the development of EC, and vice versa.

Acknowledgements

Disclosure of conflict of interest

None.

Address correspondence to: Clara Bik San Lau, Institute of Chinese Medicine, The Chinese University of Hong Kong, Shatin, New Territories, Hong Kong. E-mail: claralau@cuhk.edu.hk

References

[1] Bray F, Ferlay J, Soerjomataram I, Siegel RL, Torre LA and Jemal A. Global cancer statistics 2018: GLOBOCAN estimates of incidence and mortality worldwide for 36 cancers in 185 countries. CA Cancer J Clin 2018; 68: 394-424.

[2] National Health Commission of The People's Republic of China. Chinese guidelines for diagnosis and treatment of esophageal carcinoma 2018 (english version). Chin J Cancer Res 2019; 31: 223-258.

[3] Lagergren J, Smyth E, Cunningham D and Lagergren P. Oesophageal cancer. Lancet 2017; 390: 2383-2396.

[4] Wu SG, Zhang WW, Sun JY, Li FY, Lin Q and He ZY. Patterns of distant metastasis between histological types in esophageal cancer. Front Oncol 2018; 8: 302.

[5] Enzinger PC and Mayer RJ. Esophageal cancer. N Engl J Med 2003; 349: 2241-2252.

[6] Ai D, Zhu H, Ren W, Chen Y, Liu Q, Deng J, Ye J, Fan J and Zhao K. Patterns of distant organ metastases in esophageal cancer: a population-based study. J Thorac Dis 2017; 9: 3023-3030.

[7] Xavier JB, Young VB, Skufca J, Ginty F, Testerman T, Pearson AT, Macklin P, Mitchell A, Shmulevich I, Xie L, Caporaso JG, Crandall KA, Simone NL, Godoy-Vitorino F, Griffin TJ, Whiteson KL, Gustafson HH, Slade DJ, Schmidt TM, Walther-Antonio MRS, Korem T, Webb-Robertson BM, Styczynski MP, Johnson WE, Jobin C, Ridlon JM, Koh AY, Yu M, Kelly L and Wargo JA. The cancer microbiome: distinguishing direct and indirect effects requires a systemic view. Trends Cancer 2020; 6: 192-204.

[8] Elliott DRF, Walker AW, O'Donovan M, Parkhill J and Fitzgerald RC. A non-endoscopic device to sample the oesophageal microbiota: a case-control study. Lancet Gastroenterol Hepatol 2017; 2: 32-42.

[9] Liu AQ, Vogtmann E, Shao DT, Abnet CC, Dou HY, Qin Y, Su Z, Wei WQ and Chen W. A comparison of biopsy and mucosal swab specimens for examining the microbiota of upper gastrointestinal carcinoma. Cancer Epidemiol Biomarkers Prev 2019; 28: 2030-2037.

[10] Shao D, Vogtmann E, Liu A, Qin J, Chen W, Abnet CC and Wei W. Microbial characterization of esophageal squamous cell carcinoma and gastric cardia adenocarcinoma from a high-risk region of China. Cancer 2019; 125: 3993-4002.

[11] Snider EJ, Compres G, Freedberg DE, Khiabanian H, Nobel YR, Stump S, Uhlemann AC, Lightdale CJ and Abrams JA. Alterations to the esophageal microbiome associated with progression from Barrett's esophagus to esophageal adenocarcinoma. Cancer Epidemiol Biomarkers Prev 2019; 28: 1687-1693.

[12] Lopetuso LR, Severgnini M, Pecere S, Ponziani FR, Boskoski I, Larghi A, Quaranta G, Masucci L, Ianiro G, Camboni T, Gasbarrini A, Costamagna G, Consolandi C and Cammarota G. Esophageal microbiome signature in patients with Barrett's esophagus and esophageal adenocarcinoma. PLoS One 2020; 15: e0231789.

[13] Chen X, Winckler B, Lu M, Cheng H, Yuan Z, Yang Y, Jin L and Ye W. Oral microbiota and risk for esophageal squamous cell carcinoma in a high-risk area of China. PLoS One 2015; 10: e0143603.

[14] Nasrollahzadeh D, Malekzadeh R, Ploner A, Shakeri R, Sotoudeh M, Fahimi S, Nasseri-Moghaddam S, Kamangar F, Abnet CC, Winckler B, Islami F, Boffetta P, Brennan P, Dawsey SM and Ye W. Variations of gastric corpus microbiota are associated with early esophageal squamous cell carcinoma and squamous dysplasia. Sci Rep 2015; 5: 8820.

[15] Peters BA, Wu J, Pei Z, Yang L, Purdue MP, Freedman ND, Jacobs EJ, Gapstur SM, Hayes RB and Ahn J. Oral microbiome composition reflects prospective risk for esophageal cancers. Cancer Res 2017; 77: 6777-6787.

[16] Helmink BA, Khan MAW, Hermann A, Gopalakrishnan V and Wargo JA. The microbiome, cancer, and cancer therapy. Nat Med 2019; 25: 377-388.

[17] Zhou P, Li Z, Xu D, Wang Y, Bai Q, Feng Y, Su G, Chen P, Wang Y, Liu H, Wang X, Zhang R and Wang Y. Cepharanthine hydrochloride improves cisplatin chemotherapy and enhances immunity by regulating intestinal microbes in mice. Front Cell Infect Microbiol 2019; 9: 225.

[18] Boursi B, Mamtani R, Haynes K and Yang YX. Recurrent antibiotic exposure may promote cancer formation - another step in understanding the role of the human microbiota? Eur J Cancer 2015; 51: 2655-2664.

[19] Ohashi S, Miyamoto S, Kikuchi O, Goto T, Amanuma Y and Muto M. Recent advances from basic and clinical studies of esophageal squamous cell carcinoma. Gastroenterology 2015; 149: 1700-1715.

[20] Sougiannis AT, VanderVeen BN, Enos RT, Velazquez KT, Bader JE, Carson M, Chatzistamou I, Walla M, Pena MM, Kubinak JL, Nagarkatti M, Carson JA and Murphy EA. Impact of 5 fluorouracil chemotherapy on gut inflammation, functional parameters, and gut microbiota. Brain Behav Immun 2019; 80: 44-55.

[21] Motoori M, Yano M, Miyata H, Sugimura K, Saito T, Omori T, Fujiwara Y, Miyoshi N, Akita H, Gotoh K, Takahashi H, Kobayashi S, Noura S, Ohue M, Asahara T, Nomoto K, Ishikawa O and Sakon M. Randomized study of the effect of synbiotics during neoadjuvant chemotherapy on adverse events in esophageal cancer patients. Clin Nutr 2017; 36: 93-99.

[22] Akbar S. *Andrographis paniculata*: a review of pharmacological activities and clinical effects. Altern Med Rev 2011; 16: 66-77.

[23] Yue GGL, Lee JK, Li L, Chan KM, Wong EC, Chan JY, Fung KP, Lui VW, Chiu PW and Lau CBS. *Andrographis paniculata* elicits anti-invasion activities by suppressing TM4SF3 gene expression and by anoikis-sensitization in esophageal cancer cells. Am J Cancer Res 2015; 5: 3570-3587.

[24] Li L, Yue GGL, Lee JK, Wong EC, Fung KP, Yu J, Lau CBS and Chiu PW. The adjuvant value of *Andrographis paniculata* in metastatic esophageal cancer treatment - from preclinical perspectives. Sci Rep 2017; 7: 854.

[25] Yue GGL, Li L, Lee JK, Kwok HF, Wong EC, Li M, Fung KP, Yu J, Chan AW, Chiu PW and Lau CBS. Multiple modulatory activities of *Andrographis paniculata* on immune responses and xenograft growth in esophageal cancer preclinical models. Phytomedicine 2019; 60: 152886.

[26] Panebianco C, Adamberg K, Jaagura M, Copetti M, Fontana A, Adamberg S, Kolk K, Vilu R, Andriulli A and Pazienza V. Influence of gemcitabine chemotherapy on the microbiota of pancreatic cancer xenografted mice. Cancer Chemother Pharmacol 2018; 81: 773-782.

[27] Laukens D, Brinkman BM, Raes J, De Vos M and Vandenabeele P. Heterogeneity of the gut microbiome in mice: guidelines for optimizing experimental design. FEMS Microbiol Rev 2016; 40: 117-132.

[28] Wong SH, Zhao L, Zhang X, Nakatsu G, Han J, Xu W, Xiao X, Kwong TNY, Tsoi H, Wu WKK, Zeng B, Chan FKL, Sung JJY, Wei H and Yu J. Gavage of fecal samples from patients with colorectal cancer promotes intestinal carcinogenesis in germ-free and conventional mice. Gastroenterology 2017; 153: 1621-1633, e6.

[29] Schneider CA, Rasband WS and Eliceiri KW. NIH Image to ImageJ: 25 years of image analysis. Nat Methods 2012; 9: 671-675.

[30] Caporaso JG, Lauber CL, Walters WA, Berg-Lyons D, Lozupone CA, Turnbaugh PJ, Fierer N and Knight R. Global patterns of 16S rRNA diversity at a depth of millions of sequences per sample. Proc Natl Acad Sci U S A 2011; 108: 4516-4522.

[31] Bolyen E, Rideout JR, Dillon MR, Bokulich NA, Abnet CC, Al-Ghalith GA, Alexander H, Alm EJ, Arumugam M, Asnicar F, Bai Y, Bisanz JE, Bittinger K, Brejnrod A, Brislawn CJ, Brown CT, Callahan BJ, Caraballo-Rodríguez AM, Chase J, Cope EK, Da Silva R, Diener C, Dorrestein PC, Douglas GM, Durall DM, Duvallet C, Edwardson CF, Ernst M, Estaki M, Fouquier J, Gauglitz JM, Gibbons SM, Gibson DL, Gonzalez A, Gorlick K, Guo J, Hillmann B, Holmes S, Holste H, Huttenhower C, Huttley GA, Janssen S, Jarmusch AK, Jiang L, Kaehler BD, Kang KB, Keefe CR, Keim P, Kelley ST, Knights D, Koester I, Kosciolek T, Kreps J, Langille MGI, Lee J, Ley R, Liu YX, Loftfield E, Lozupone C, Maher M, Marotz C, Martin BD, McDonald D, McIver LJ, Melnik AV, Metcalf JL, Morgan SC, Morton JT, Naimey AT, Navas-Molina JA, Nothias LF, Orchanian SB, Pearson T, Peoples SL, Petras D, Preuss ML, Pruesse E, Rasmussen LB, Rivers A, Robeson MS 2nd, Rosenthal P, Segata N, Shaffer M, Shiffer A, Sinha R, Song SJ, Spear JR, Swafford AD, Thompson LR, Torres PJ, Trinh P, Tripathi A, Turnbaugh PJ, Ul-Hasan S, van der Hooft JJJ, Vargas F, Vázquez-Baeza Y, Vogtmann E, von Hippel M, Walters W, Wan Y, Wang M, Warren J, Weber KC, Williamson CHD, Willis AD, Xu ZZ, Zaneveld JR, Zhang Y, Zhu Q, Knight R and Caporaso JG. Reproducible, interactive, scalable and extensible microbiome data science using QIIME 2. Nat Biotechnol 2019; 37: 852-857.

[32] Martin M. Cutadapt removes adapter sequences from high-throughput sequencing reads. EMBnet J 2011; 17: 10-12.

[33] Rognes T, Flouri T, Nichols B, Quince C and Mahé F. VSEARCH: a versatile open source tool for metagenomics. PeerJ 2016; 4: e2584.

[34] Amir A, McDonald D, Navas-Molina JA, Kopylova E, Morton JT, Zech Xu Z, Kightley EP, Thompson LR, Hyde ER, Gonzalez A and Knight R. Deblur rapidly resolves single-nucleotide community sequence patterns. mSystems 2017; 2: e00191-16.

[35] Bokulich NA, Kaehler BD, Rideout JR, Dillon M, Bolyen E, Knight R, Huttley GA and Gregory Caporaso J. Optimizing taxonomic classification of marker-gene amplicon sequences with QIIME 2's q2-feature-classifier plugin. Microbiome 2018; 6: 90.

[36] Quast C, Pruesse E, Yilmaz P, Gerken J, Schweer T, Yarza P, Peplies J and Glöckner FO. The SILVA ribosomal RNA gene database project: improved data processing and web-based tools. Nucleic Acids Res 2013; 41: D590-D596.

[37] Katoh K, Misawa K, Kuma K and Miyata T. MAFFT: a novel method for rapid multiple sequence alignment based on fast Fourier transform. Nucleic Acids Res 2002; 30: 3059-3066.

[38] Price MN, Dehal PS and Arkin AP. FastTree 2 - approximately maximum-likelihood trees for large alignments. PLoS One 2010; 5: e9490.

[39] Mandal S, Van Treuren W, White RA, Eggesbø M, Knight R and Peddada SD. Analysis of composition of microbiomes: a novel method for studying microbial composition. Microb Ecol Health Dis 2015; 26: 27663.

[40] Bardou P, Mariette J, Escudié F, Djemiel C and Klopp C. jvenn: an interactive Venn diagram viewer. BMC Bioinformatics 2014; 15: 293.

[41] Langille MG, Zaneveld J, Caporaso JG, McDonald D, Knights D, Reyes JA, Clemente JC, Burkepile DE, Vega Thurber RL, Knight R, Beiko RG and Huttenhower C. Predictive functional profiling of microbial communities using 16S rRNA marker gene sequences. Nat Biotechnol 2013; 31: 814-821.

[42] McDonald D, Price MN, Goodrich J, Nawrocki EP, DeSantis TZ, Probst A, Andersen GL, Knight R and Hugenholtz P. An improved Greengenes taxonomy with explicit ranks for ecological and evolutionary analyses of bacteria and archaea. ISME J 2012; 6: 610-618.

[43] Parks DH, Tyson GW, Hugenholtz P and Beiko RG. STAMP: statistical analysis of taxonomic and functional profiles. Bioinformatics 2014; 30: 3123-3124.

[44] Szadvari I, Krizanova O and Babula P. Athymic nude mice as an experimental model for cancer treatment. Physiol Res 2016; 65: S441-S453.

[45] Schmidt TS, Hayward MR, Coelho LP, Li SS, Costea PI, Voigt AY, Wirbel J, Maistrenko OM, Alves RJ, Bergsten E, de Beaufort C, Sobhani I, Heintz-Buschart A, Sunagawa S, Zeller G, Wilmes P and Bork P. Extensive transmission of microbes along the gastrointestinal tract. Elife 2019; 8: e42693.

[46] Heshiki Y, Vazquez-Uribe R, Li J, Ni Y, Quainoo S, Imamovic L, Li J, Sørensen M, Chow BKC, Weiss GJ, Xu A and Sommer MOA. Predictable modulation of cancer treatment outcomes by the gut microbiota. Microbiome 2020; 8: 28.

[47] Gao H, Shu Q, Chen J, Fan K, Xu P, Zhou Q, Li C and Zheng H. Antibiotic exposure has sex-dependent effects on the gut microbiota and metabolism of short-chain fatty acids and amino acids in mice. mSystems 2019; 4: e00048-19.

[48] Song W, Anselmo AC and Huang L. Nanotechnology intervention of the microbiome for cancer therapy. Nat Nanotechnol 2019; 14: 1093-1103.

[49] Christensen H, Kuhnert P, Nørskov-Lauritsen N, Planet PJ and Bisgaard M. The family Pasteurellaceae. The Prokaryotes - Gammaproteobacteria. In: Rosenberg E, DeLong EF, Lory S, Stackebrandt E and Thompson F editors. Delhi: Springer-Verlag Berlin Heidelberg; 2014. pp. 535-564.

[50] Yang J, McDowell A, Kim EK, Seo H, Lee WH, Moon CM, Kym SM, Lee DH, Park YS, Jee YK and Kim YK. Development of a colorectal cancer diagnostic model and dietary risk assessment through gut microbiome analysis. Exp Mol Med 2019; 51: 1-15.

[51] Olson SH, Satagopan J, Xu Y, Ling L, Leong S, Orlow I, Saldia A, Li P, Nunes P, Madonia V, Allen PJ, O'Reilly E, Pamer E and Kurtz RC. The oral microbiota in patients with pancreatic cancer, patients with IPMNs, and controls: a pilot study. Cancer Causes Control 2017; 28: 959-969.

[52] Yu C, Su Z, Li Y, Li Y, Liu K, Chu F, Liu T, Chen R and Ding X. Dysbiosis of gut microbiota is associated with gastric carcinogenesis in rats. Biomed Pharmacother 2020; 126: 110036.

[53] Zhang L, Wu YN, Chen T, Ren CH, Li X and Liu GX. Relationship between intestinal microbial dysbiosis and primary liver cancer. Hepatobiliary Pancreat Dis Int 2019; 18: 149-157.

[54] Zhang WQ, Zhao SK, Luo JW, Dong XP, Hao YT, Li H, Shan L, Zhou Y, Shi HB, Zhang ZY, Peng CL and Zhao XG. Alterations of fecal bacterial communities in patients with lung cancer. Am J Transl Res 2018; 10: 3171-3185.

[55] Yang Y, Misra BB, Liang L, Bi D, Weng W, Wu W, Cai S, Qin H, Goel A, Li X and Ma Y. Integrated microbiome and metabolome analysis reveals a novel interplay between commensal bacteria and metabolites in colorectal cancer. Theranostics 2019; 9: 4101-4114.

[56] Ferreira RM, Pereira-Marques J, Pinto-Ribeiro I, Costa JL, Carneiro F, Machado JC and Figueiredo C. Gastric microbial community profiling reveals a dysbiotic cancer-associated microbiota. Gut 2018; 67: 226-236.

[57] Faubert B, Solmonson A and DeBerardinis RJ. Metabolic reprogramming and cancer progression. Science 2020; 368: eaaw5473.

[58] Dapito DH, Mencin A, Gwak GY, Pradere JP, Jang MK, Mederacke I, Caviglia JM, Khiabanian H, Adeyemi A, Bataller R, Lefkowitch JH, Bower M, Friedman R, Sartor RB, Rabadan R and Schwabe RF. Promotion of hepatocellular carcinoma by the intestinal microbiota and TLR4. Cancer Cell 2012; 21: 504-516.

[59] Thomas RM, Gharaibeh RZ, Gauthier J, Beveridge M, Pope JL, Guijarro MV, Yu Q, He Z, Ohland C, Newsome R, Trevino J, Hughes SJ, Reinhard M, Winglee K, Fodor AA, Zajac-Kaye M and Jobin C. Intestinal microbiota enhances pancreatic carcinogenesis in preclinical models. Carcinogenesis 2018; 39: 1068-1078.

[60] Zhan Y, Chen PJ, Sadler WD, Wang F, Poe S, Núñez G, Eaton KA and Chen GY. Gut microbiota protects against gastrointestinal tumorigenesis caused by epithelial injury. Cancer Res 2013; 73: 7199-7210.

[61] Schuijt TJ, Lankelma JM, Scicluna BP, de Sousa e Melo F, Roelofs JJ, de Boer JD, Hoogendijk AJ, de Beer R, de Vos A, Belzer C, de Vos WM, van der Poll T and Wiersinga WJ. The gut microbiota plays a protective role in the host defence against pneumococcal pneumonia. Gut 2016; 65: 575-583.

[62] Coryell M, McAlpine M, Pinkham NV, McDermott TR and Walk ST. The gut microbiome is required for full protection against acute arsenic toxicity in mouse models. Nat Commun 2018; 9: 5424.

[63] Torres PJ, Ho BS, Arroyo P, Sau L, Chen A, Kelley ST and Thackray VG. Exposure to a healthy gut microbiome protects against reproductive and metabolic dysregulation in a PCOS mouse model. Endocrinology 2019; 160: 1193-1204.

[64] Allegretti JR, Mullish BH, Kelly C and Fischer M. The evolution of the use of faecal microbiota transplantation and emerging therapeutic indications. Lancet 2019; 394: 420-431.

[65] Chen D, Wu J, Jin D, Wang B and Cao H. Fecal microbiota transplantation in cancer management: current status and perspectives. Int J Cancer 2019; 145: 2021-2031.

[66] Yuan L, Zhang S, Li H, Yang F, Mushtaq N, Ullah S, Shi Y, An C and Xu J. The influence of gut microbiota dysbiosis to the efficacy of 5-Fluorouracil treatment on colorectal cancer. Biomed Pharmacother 2018; 108: 184-193.

[67] Nagpal R and Yadav H. Bacterial translocation from the gut to the distant organs: an overview. Ann Nutr Metab 2017; 71 Suppl 1: 11-16.

[68] Viaud S, Saccheri F, Mignot G, Yamazaki T, Daillère R, Hannani D, Enot DP, Pfirschke C, Engblom C, Pittet MJ, Schlitzer A, Ginhoux F, Apetoh L, Chachaty E, Woerther PL, Eberl G, Bérard M, Ecobichon C, Clermont D, Bizet C, Gaboriau-Routhiau V, Cerf-Bensussan N, Opolon P, Yessaad N, Vivier E, Ryffel B, Elson CO, Doré J, Kroemer G, Lepage P, Boneca IG, Ghiringhelli F and Zitvogel L. The intestinal microbiota modulates the anticancer immune effects of cyclophosphamide. Science 2013; 342: 971-976.

[69] Pushalkar S, Hundeyin M, Daley D, Zambirinis CP, Kurz E, Mishra A, Mohan N, Aykut B, Usyk M, Torres LE, Werba G, Zhang K, Guo Y, Li Q, Akkad N, Lall S, Wadowski B, Gutierrez J, Kochen Rossi JA, Herzog JW, Diskin B, Torres-Hernandez A, Leinwand J, Wang W, Taunk PS, Savadkar S, Janal M, Saxena A, Li X, Cohen D, Sartor RB, Saxena D and Miller G. The pancreatic cancer microbiome promotes oncogenesis by induction of innate and adaptive immune suppression. Cancer Discov 2018; 8: 403-416.

[70] Cheung MK, Yue GGL, Chiu PWY and Lau CBS. A review of the effects of natural compounds, medicinal plants, and mushrooms on the gut microbiota in colitis and cancer. Front Pharmacol 2020; 11: 744.

[71] Feng W, Ao H, Peng C and Yan D. Gut microbiota, a new frontier to understand traditional Chinese medicines. Pharmacol Res 2019; 142: 176-191.

[72] Islam MT, Ali ES, Uddin SJ, Islam MA, Shaw S, Khan IN, Saravi SSS, Ahmad S, Rehman S, Gupta VK, Găman MA, Găman AM, Yele S, Das AK, de Castro E Sousa JM, de Moura Dantas SMM, Rolim HML, de Carvalho Melo-Cavalcante AA, Mubarak MS, Yarla NS, Shilpi JA, Mishra SK, Atanasov AG and Kamal MA. Andrographolide, a diterpene lactone from *Andrographis paniculata* and its therapeutic promises in cancer. Cancer Lett 2018; 420: 129-145.

[73] Cammarota G, Ianiro G, Tilg H, Rajilić-Stojanović M, Kump P, Satokari R, Sokol H, Arkkila P, Pintus C, Hart A, Segal J, Aloi M, Masucci L, Molinaro A, Scaldaferri F, Gasbarrini G, Lopez-Sanroman A, Link A, de Groot P, de Vos WM, Högenauer C, Malfertheiner P, Mattila E, Milosavljević T, Nieuwdorp M, Sanguinetti M, Simren M and Gasbarrini A; European FMT Working Group. European consensus conference on faecal microbiota transplantation in clinical practice. Gut 2017; 66: 569-580.